

A SCALABLE SIX-AXIS ELECTROMAGNETICALLY-DRIVEN NANOPOSITIONER FOR NANOMANUFACTURING

Dariusz Golda¹, and Martin L. Culpepper¹

¹Department of Mechanical Engineering
Massachusetts Institute of Technology
Cambridge, MA, USA

ABSTRACT

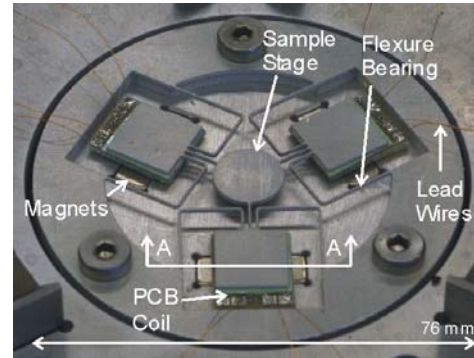
This paper presents the design and demonstrated performance of a low-cost, centimeter-scale, six-axis nanopositioner driven by electromagnetic actuators with applications in nanomanufacturing and scanning-probe microscopy. The planar device can operate linearly with a range-of-motion of nearly 8 micrometers in the x-, y- and z- directions with a first resonance of 120 Hz. Sensor-limited repeatability of better than 20nm has been demonstrated, while the minimum measured step size is 10nm. The system is a first step toward the design of a high-speed meso-scale six-axis device. As such, it can be scaled down to several millimeters in size, enabling high-speed and precise positioning of small samples such as probe tips and thin-film materials.

INTRODUCTION

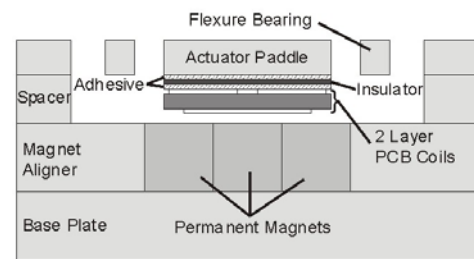
Multi-axis meso-scale nanopositioners can enable high-speed and precise positioning and measurement in the biological sciences, data storage, probing equipment for nano-scale measurements, and more recently, nanomanufacturing processes [1-5]. Emerging applications in these fields would benefit from portable, multi-axis, nanometer-level positioning over tens-of-microns at speeds of hundreds to thousands of Hertz. Several design challenges must be overcome in order to achieve high-speed multi-axis sample positioning using a meso-scale device: 1) multi-axis actuator and bearing design and integration; 2) position sensing for feedback control; 3) power dissipation; 4) sample integration. We have designed, constructed, and tested a low-cost, centimeter-scale 6-axis nanopositioner of planar geometry as a potential solution to the first design challenge. The system is a first step towards the design goal of a meso-scale system.

DESIGN OF THE PROTOTYPE SYSTEM

The nanopositioner is shown in Fig. 1a), while cross section A-A depicting the actuator layers is shown in Fig. 1b).



(a)



(b)

FIGURE 1. a) Bench-level prototype nanopositioner. b) Cross-section A-A of the nanopositioner showing actuator components.

The device operates in open-loop, and is comprised of a planar, spatially compliant 6061 aluminum flexure bearing [6], and three sets of two-axes moving-coil actuators. The system has six total actuator inputs, and six possible position outputs. The aluminum flexure arms are approximately 0.82mm thick and 0.64mm wide. The actuators consist of planar-coils fabricated on a printed circuit board (PCB) suspended above a set of three alternating-pole permanent magnets. An aluminum spacer is used to achieve the correct gap between the PCB coils and the permanent magnet structure. The PCB coils are bonded to the underside of the flexure bearing actuator paddles, and protected from shorting to the aluminum via plastic insulator layer. Thin 36-gauge insulated lead wires are used to supply the moving coils with current while adding negligible stiffness to the structure. The three-way symmetric design

[6] and relatively small out-of-plane profile mitigate thermal errors in the stage position.

When powered, the actuators apply forces to deflect the flexure bearing. Electromagnetic simulations have been used to predict the force output of the actuators as a function of current. Assuming linearity, the set of input currents required to achieve some static output state \mathbf{x} is related through:

$$\mathbf{i} = (TK_a)^{-1} K\mathbf{x} \quad (1)$$

The actuator matrix K_a is derived from the electromagnetic analysis, and relates the command currents to actuator forces. This is multiplied by the kinematic transformation matrix T that maps forces at the actuator location to the structure. The structural stiffness matrix K is then multiplied to map the applied force on the structure to the output displacement. In practice, this input-output mapping is measured and results in a linear calibration matrix.

The flexure dimensions were designed such that the force-limited system has a range of motion of roughly 10 μm when the actuator coils are powered with the maximum sustainable current of 500mA. The resulting first mechanical natural frequency of the system is roughly 125 Hz, as computed using finite element analysis (FEA). Figure 2 shows the first mode of the system, which is tilting out-of-the-plane.

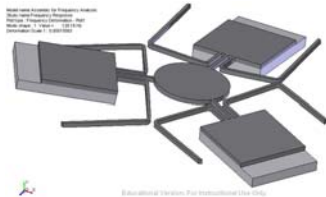


FIGURE 2. First mode of the nanopositioner at 125Hz as computed using FEA.

The planar geometry of the flexure bearing and coil actuators enable scaling of the system via lithographic microfabrication. Miniaturization to the meso-scale would result in improved performance through: a) reduced thermal error; b) increased natural frequency; c) more efficient coil actuators.

EXPERIMENTAL RESULTS

The prototype centimeter-scale nanopositioner has been calibrated and tested using a set of six capacitance probes and target fixture. Data was

collected with a DSpace 16 bit real-time data acquisition system operating at 1000Hz. Lion Precision capacitance probes were used to obtain position measurement from the multi-axis probe target. A custom-built 6-channel voltage-current amplifier was used to power the coils. Figure 3 shows the nanopositioner with capacitance probe target mounted to the sample stage, and the six-probe fixture. In practical applications a smaller target/metrology system would be used. The relatively large size of the target used in our experiment is as small as permitted by our current sensing/data acquisition system.

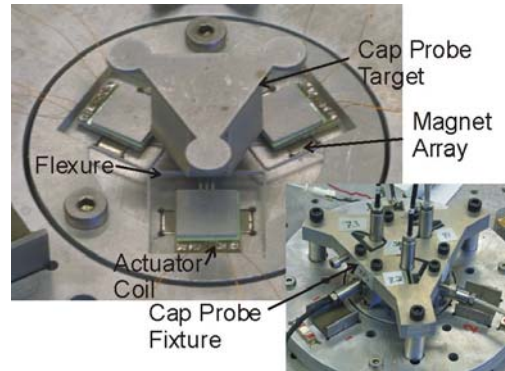


FIGURE 3. Nanopositioner with capacitance probes and measurement target.

The range-of-motion of the positioner is measured to be close to ± 4 microns in each of the X-, Y-, and Z-directions. Figures 4 and 5 show the input-output relationship of the system in the x- and z- direction, which is limited by the current-carrying capability of the PCB coils.

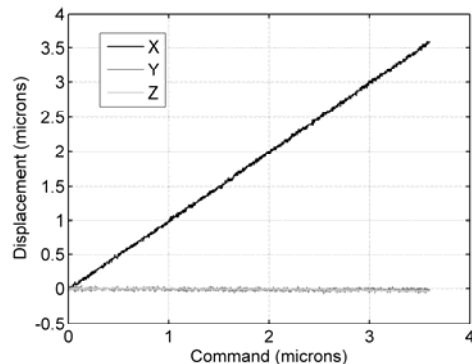


Figure 4. Measured vs. commanded displacement in the x-direction.

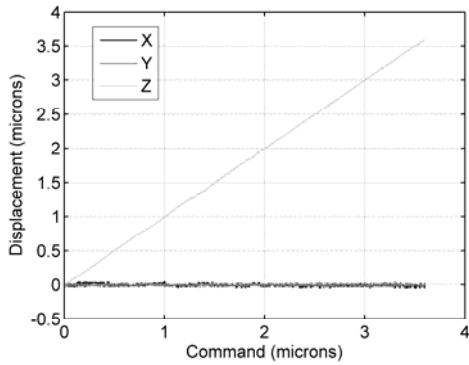


FIGURE 5. Measured vs. commanded displacement in the z-direction

The dynamics response of the system has been measured by referencing one capacitance probe off the sample stage without using the probe target which adds considerable mass to the system. Figure 6 shows the frequency response of the system in the out-of-plane direction (z-direction). The predicted out-of-plane first natural frequency of 125 Hz closely matches the first measured peak at 120 Hz.

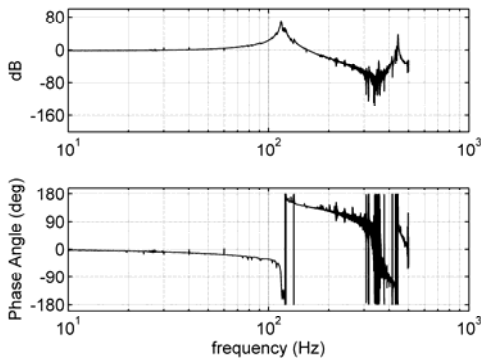


FIGURE 6. Dynamic response in the z-direction without probe target.

The in-plane repeatability and step response was measured with the capacitance probe target and 6-probe setup. The system was commanded to step in the x-direction by 600nm and return. The measured x-, y-, and z- motions are shown in Fig. 7. The under-damped system tends to ring for a few seconds in response to the step input in all three axes as a result of the tilting mode harmonics. The figure indicates that although the system rings, the repeatability is on the order of the measurement noise, which in this case is roughly 20nm.

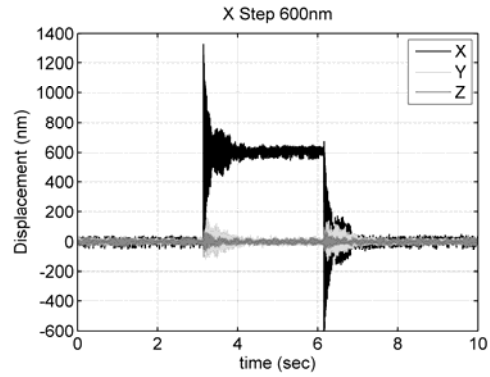


FIGURE 7. Nanopositioner response to a 600nm step input in the X-direction with 6-axis capacitance probe target.

Out-of-plane repeatability and step response was also measured, but without the capacitance probe target. In this case, a single probe referenced directly to the sample stage surface. Figures 8-10 show the results of commanded 10nm, 100nm, and 1000nm steps. Again, the under-damped system overshoots the target step height, but the oscillations damp out in less than 0.5 seconds. The oscillations could be damped in open-loop using techniques such as input pre-filtering, or by adding visco-elastic elements. The data indicates that the repeatability of the system is approximately that of the noise floor of 20nm in all three cases.

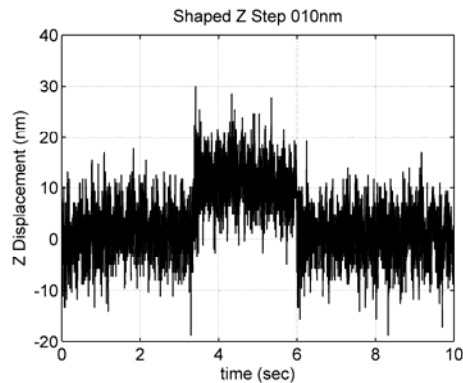


FIGURE 8. Nanopositioner response to a 10nm step in the z-direction without the capacitance probe target.

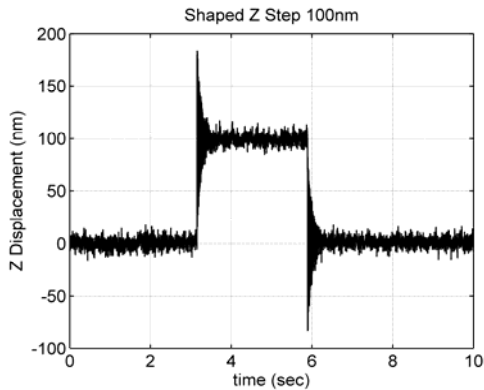


FIGURE 9. Response of the nanopositioner to a 100nm step in the z-direction, without the capacitance probe target.

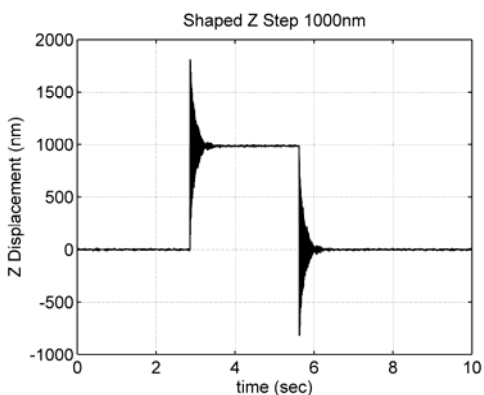


FIGURE 10. Repeatability of 1000nm step in the z-direction without 6-axis probe target.

In order to demonstrate the full three-dimensional capabilities of the nanopositioner, the system was commanded to traverse a 1 μm spiral trajectory in open-loop. The six-probe fixture and probe target were used to record position. The commanded and measured data is plotted in Fig. 11.

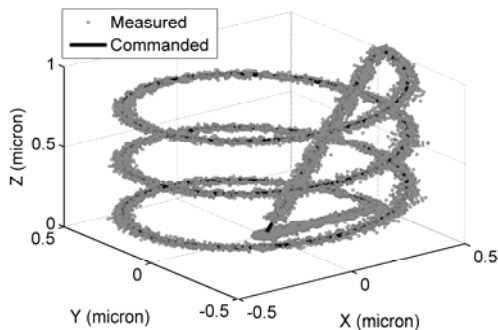


FIGURE 11. Measured trajectory of the nanopositioner when commanded to follow a 3-loop spiral trajectory with diameter and total traversed height of 1000nm.

The data indicates that the positioner follows the desired trajectory to within the noise of the measurement system.

CONCLUSION

A centimeter-scale, electromagnetically-driven nanopositioner has been designed and tested to have 8 microns range-of-motion and repeatability of better than 20nm. The low-cost prototype nanopositioner design is scalable down to the millimeter size through microfabrication. Miniaturization would lead to several performance benefits including increased bandwidth, increased coil current density, and favorable thermal performance. Target applications for the meso-scale system include high-throughput nanomanufacturing and scanning probe microscopy. The prototype is currently being integrated into a bench-top electric-pen lithography system for demonstration of low-cost nanomanufacturing.

REFERENCES

1. Lutwyche, M., et al., "Planar Micromagnetic X/Y/Z Scanner with Five Degrees of Freedom," presented at Proceedings of the 194th Meeting of the Electrochemical Society, Boston, 1998.
2. Rothuizen, H., et al., "Compact Copper/Epoxy-Based Electromagnetic Scanner for Scanning Probe Applications," presented at 15th IEEE International Conference on Micro Electro Mechanical Systems MEMS 2002, Jan 20-24 2002, Las Vegas, NV, 2002.
3. Rothuizen, H., et al., "Fabrication of a Micromachined Magnetic X/Y/Z Scanner for Parallel Scanning Probe Applications," *Microelectronic Engineering*, vol. 53, pp. 509-512, 2000.
4. Pantazi, A., et al., "A Servomechanism for a Micro-Electromechanical-System-Based Scanning-Probe Data Storage Device," *Nanotechnology*, vol. 15, pp. 612-621, 2004.
5. Malshe, A. P., et al., "Investigation of Nanoscale Electro Machining (Nano-Em) in Dielectric Oil," presented at 55th CIRP General Assembly, Antalya, Turkey, 2005.
6. Culpepper, M. L. and Anderson, G., "Design of a Low-Cost Nano-Manipulator Which Utilizes a Monolithic, Spatial Compliant Mechanism," *Precision Engineering*, vol. 28, pp. 469-482, 2004.